Evaluation of cobalt(III) tetramethylchiroporphyrin as an analytical reagent for the determination of enantiomer composition of primary amines and aziridines by ^{1}H NMR spectroscopy

Jean-Pierre Simonato,†[a] Sabrina Chappellet,[a] Jacques Pécaut,[a] Paul Baret[b] and Jean-Claude Marchon*[a]

[a] *Laboratoire de Chimie Inorganique et Biologique, (CNRS UMR 5046), Département de Recherche Fondamentale sur la Matière Condensée, CEA-Grenoble, 38054 Grenoble, France. E-mail: jcmarchon@cea.fr; Fax: +33 4 76 88 54 97*

[b] *Laboratoire de Chimie Biomimétique, (LEDSS, CNRS UMR 5616), Université de Grenoble 1, BP 53, 38041 Grenoble, France*

Received (in Strasbourg, France) 3rd January 2001, Accepted 19th February 2001

The irreversible reaction of chlorocobalt(III) tetramethylchiroporphyrin CoCl(TMCP), **1**, with nitrogen donor ligands L, such as primary amines and aziridines, in deuterated chloroform solution at room temperature gives cationic bis-adducts of the type $[Co(L)_2(TMCP)]^+Cl^-$ in quantitative yields. Upon binding to the chiral host **1**, the protons of L experience a shielding by the porphyrin, and several of their ^{1}H NMR signals are shifted to a vacant spectral window upfield of tetramethylsilane ($0 > \delta > -6.5$). The coordinated (*R*) and (*S*) enantiomers show well-resolved signatures at 200 MHz, allowing their relative concentrations to be readily determined by peak integration. Racemic amine derivatives such as 2-butylamine, 1-aminoindane, α-amino-γ-butyrolactone, 1-phenylethylamine, 2-aminomethoxypropane and 1-(1-naphthyl)ethylamine bind to **1** in $CDCl_3$ solution without detectable kinetic resolution, affording a 1 : 1 concentration ratio of the two cobalt-bound enantiomers (R_{Co}) and (S_{Co}), as measured by ^{1}H NMR. Aziridines such as ethyl 2-aziridinecarboxylate and 2-aziridinemethanol behave in an analogous manner. Standard solutions of 1-(1-naphthyl)ethylamine covering a range of enantiomer compositions $x = (R)/[(R) + (S)]$ ($x = 0, 0.1, 0.25, 0.5, 0.75, 0.9, 1$) were analyzed using **1** as a chiral NMR shift reagent. The bound enantiomer composition values $y = (R_{Co})/[(R_{Co}) + (S_{Co})]$ measured by NMR were in good agreement with those of the standard solutions, and the calibration curve $y = f(x)$ was linear in the range $0 \leqslant x \leqslant 1$, within experimental error. These features of **1** as a chiral analytical reagent may prove suitable for the accurate determination of a wide range of enantiomeric excesses of amines and aziridines. The crystal structures of $\{Co[(R)\text{-}1\text{-}(1\text{-naphthyl})ethylamine]_2(TMCP)\}^+Cl^-$ and $\{Co[(R)\text{-}2\text{-butylamine}]_2(TMCP)\}^+Cl^-$ are described.

The need for reliable analytical techniques for the determination of enantiomer composition is becoming increasingly important with the development of chirotechnologies.[1] Accurate and practical methods of chiral analysis are important in the pharmaceutical industries, notably for licensing drugs. Among the presently available techniques, chiral chromatography has gained considerable popularity due to its wide applicability and ease of operation. ^{1}H NMR spectroscopy is another potentially advantageous method since it does not require specific instrumentation and is fast. However, NMR is an achiral technique that does not distinguish enantiomers, and therefore chemical modification of the enantiomer mixture is usually necessary prior to analysis itself. In the case of optically active amines, a number of chiral auxiliaries have been proposed for this purpose,[2] and they are usually classified as derivatizing agents,[3] solvating agents,[4] and lanthanide shift reagents.[5] Adduct formation of amines with chiral transition metal complexes has also been used for their chiral analysis by NMR.[6] A crucial prerequisite is that the concentration ratio of diastereomers accurately reflects that of the starting enantiomer mixture, that is, kinetic resolution does not occur in the derivatization step.

In a previous investigation, we have shown that the chlorocobalt(III) complex of tetramethylchiroporphyrin, **1**, is a potential chiral NMR shift reagent for aliphatic amines.[7] A key structural feature of **1** is the presence of a groove of 3–4 Å width on each face of the porphyrin, which can accommodate an axial ligand in a chiral microenvironment. This diamagnetic cobalt(III) complex reacts with chiral aliphatic amines L in CD_2Cl_2 solution at room temperature to give the cationic bis-amine adducts $[CoL_2(TMCP)]^+$ in quantitative yields. Several ^{1}H resonances of the axial ligands L are shifted to a vacant spectral window upfield of tetramethylsilane ($0 > \delta > -6$). The coordinated (*R*) and (*S*) enantiomers showed well-resolved signatures at 200 MHz, allowing their

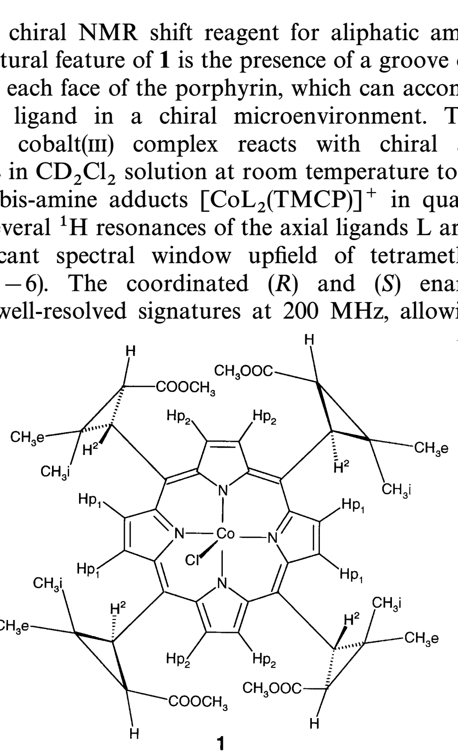

1

---

† Present address: Rhodia Recherches, 85 rue des Frères Perret, 69192 Saint Fons cedex, France.

DOI: 10.1039/b100268f

relative concentrations to be readily determined by peak integration. With (R,S)-2-butylamine, 2-pentylamine or 2-hexylamine, statistical ratios of 1 : 2 : 1 were found for the concentrations of the three species $[\mathrm{Co}(R)(R)]^+$, $[\mathrm{Co}(R)(S)]^+$ and $[\mathrm{Co}(S)(S)]^+$.[8] This absence of kinetic resolution was accounted for by the extremely slow dissociation kinetics of the axial ligands, which are not at equilibrium with the cobalt(III) host. In contrast, we have observed notable kinetic resolution in the binding of chiral alcohols, such as 2-octanol, to the carbonylruthenium(II) analog of **1**.[9]

These observations led us to the conclusion that the extreme kinetic inertness of cobalt(III) in its TMCP complexes could be utilized for the chiral analysis of amines. With this purpose in mind, we have now extended our NMR studies to a series of racemic amines and aziridines, and to a large range of enantiomeric ratios in the case of 1-(1-naphthyl)ethylamine. We have checked that the distribution of enantiomer ligands in the product complexes consistently matches that of the starting enantiomer mixture within experimental error. We have also solved the crystal structures of the bis (R)-1-(1-naphthyl)ethylamine and bis (R)-2-butylamine adducts of $\mathrm{Co(III)(TMCP)}^+$, and correlated these with the solution structures deduced from NMR. Herein, we report the results of these investigations.

Results and discussion

^{1}H NMR spectra of the bis-adducts of enantiopure and racemic 1-(1-naphthyl)ethylamine

Addition of enantiopure (R)- or (S)-1-(1-naphthyl)ethylamine (6 equiv.) to a solution of CoCl(TMCP) in $\mathrm{CDCl_3}$ afforded the $[\mathrm{Co}(R)(R)]^+$ and $[\mathrm{Co}(S)(S)]^+$ adducts, the ^{1}H NMR spectra of which are illustrated in Fig. 1. Amine complexation is accompanied by a change in effective symmetry from C_2 in **1** to D_2 in the bis-amine adduct, as seen by the presence of a single set of resonances for the *meso* substituents and two singlets for the β-pyrrole protons (Table 1). The opposite absolute configurations of the two bound enantiomers result in different spectral signatures for the chiral host. A notable difference is seen in the separation of the two β-pyrrole singlets, which is larger for the $[\mathrm{Co}(R)(R)]^+$ complex than for $[\mathrm{Co}(S)(S)]^+$ (0.52 and 0.21 ppm, respectively, *cf.* Table 1).

Assignments of the resonances of the axial amine ligands were obtained by 2D ^{1}H NMR experiments and they are collected in Table 2. Upon adduct formation, the resonances of the ligand protons are spread across a 13 ppm window (+7 to −6 ppm *vs.* TMS) and shifted upfield as a result of the strong shielding effect of the porphyrin moiety.[7] The shift is largest for those ligand protons nearest the macrocycle and close to the porphyrin normal (Fig. 2). The protons of the naphthyl groups are spread from 7.21 to 3.30 ppm. The protons of the amine group, Ha and Hb exhibit notably different chemical shifts, $\Delta\delta \approx 0.5$. The resonance at lower field is presumably that of the N–H proton involved in a hydrogen bond with one carbonyl group of the *meso* substituents, as seen in the crystal structure of $\{\mathrm{Co}[(R)\text{-1-(1-naphthyl)ethylamine}]_2(\mathrm{TMCP})\}^+\mathrm{Cl}^-$, **2** (*vide infra*). The chemical shift differences between the coordinated enantiomers, collected in Table 2, are largest for the protons located near the center of the porphyrin ring, particularly for the methyl group ($\Delta\delta \approx 0.44$ ppm). This wide diastereomer dispersion, and the large intensity of the methyl peak (3 protons), are particularly suitable for an accurate and sensitive determination of the enantiomer composition by integration. In contrast, the dia-

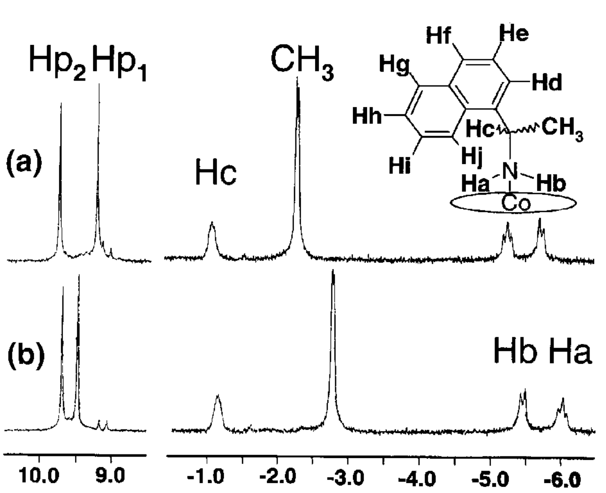

Fig. 1 200 MHz ^{1}H NMR spectra of enantiopure 1-(1-naphthyl)ethylamine coordinated to $[\mathrm{Co^{III}(TMCP)}]^+$ in $\mathrm{CDCl_3}$ at 25 °C: (a) (R)-1-(1-naphthyl)ethylamine, (b) (S)-1-(1-naphthyl)ethylamine. The small signals near 9.2 ppm are due to a tiny amount of $\mathrm{H_2TMCP}$.

Table 1 ^{1}H NMR chemical shifts of the porphyrin protons in CoCl(TMCP)-derivatized 1-(1-naphthyl)ethylamine enantiomers

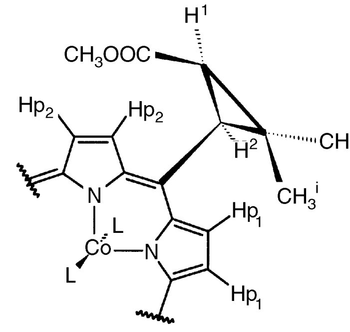

Proton	$[\mathrm{Co}(R)(R)]^+$	$[\mathrm{Co}(S)(S)]^+$
$\mathrm{Hp_2}$	9.76	9.68
$\mathrm{Hp_1}$	9.24	9.47
$\mathrm{H^2}$	4.87	4.94
	(J = 8.8 Hz)	(J = 9.2 Hz)
$\mathrm{COOCH_3}$	3.05	2.53
$\mathrm{H^1}$	2.81	2.73
	(J = 8.8 Hz)	(J = 9.2 Hz)
$\mathrm{CH_3}^\mathrm{e}$	1.98	1.97
$\mathrm{CH_3}^\mathrm{i}$	0.17	0.88

Table 2 ^{1}H NMR chemical shifts of 1-(1-naphthyl)ethylamine enantiomers derivatized by CoCl(TMCP), and their diastereomeric dispersions

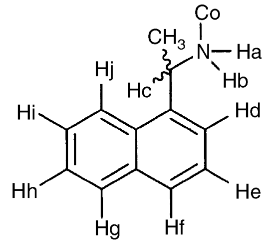

Proton	$[\mathrm{Co}(R)(R)]^+$	$[\mathrm{Co}(S)(S)]^+$	$\lvert\Delta\delta\rvert$
$\mathrm{CH_3}$	−2.34	−2.78	0.44
Ha	−5.75	−6.01	0.26
Hb	−5.27	−5.45	0.18
Hc	−1.16	−1.16	0.00
Hd	3.30	3.40	0.10
He	7.11	6.73	0.38
Hf	7.21	7.17	0.04
Hg/Hh	6.94	6.99	0.05
Hi	6.31	6.37	0.06
Hj	5.30	5.27	0.03

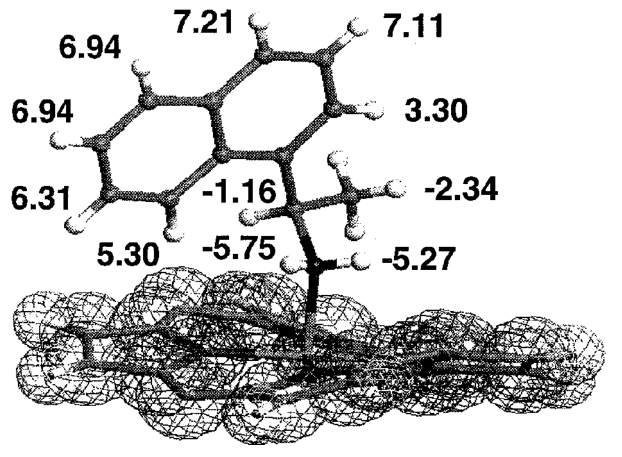

Fig. 2 A schematic illustration of the (*R*)-1-(1-naphthyl)ethylamine ligand axially coordinated to the Co(III) chiroporphyrin, drawn from the atomic coordinates of the $[Co(R)(R)]^+$ complex. The chemical shifts of the (*R*)-1-(1-naphthyl)ethylamine protons are indicated. *Meso* groups are omitted and only one of the two identical faces is shown for clarity.

stereomer dispersion is vanishingly small for the methine proton Hc. This suggests that Hc is kept in the same position within the chiral host in both enantiomer adducts. The solid state structures of **2** and of the corresponding (*R*)-2-butylamine adduct (*vide infra*) show the presence of a weak Hc···O=C hydrogen bond, which has also been seen earlier in the structure of the (*S*)-2-butylamine adduct.[7] This Hc···O=C hydrogen bond, therefore, is likely to exist in all amine bis-adducts of **1**, including the [(*S*)-1-(1-naphthyl)ethylamine] complex.

When a racemic mixture of 1-(1-naphthyl)ethylamine was added to **1**, only two sets of peaks were observed in the higher field region of the spectrum. Apparently, the signals of the (*R*)-amine in the mixed complex $[Co(R)(S)]^+$ overlap with those due to $[Co(R)(R)]^+$, and those of the (*S*)-amine in $[Co(R)(S)]^+$ with those of $[Co(S)(S)]^+$.

^{1}H NMR spectra of the bis-adducts of *rac*- and (*S*)-ethyl 2-aziridinecarboxylate

Addition of *rac*-ethyl 2-aziridinecarboxylate to a solution of **1** also results in an immediate symmetry change of the ^{1}H NMR spectrum, reflecting the formation of bis-adducts. In this case, the protons of the three-membered rings are again strongly shielded and the resonances of each bound enantiomer are not very sensitive to the absolute configuration of the second axial ligand *trans* to it. The signals of the coordinated aziridines appear mainly upfield of TMS, except that of the ethyl group which lies at the periphery of the aromatic ring. 2D ^{1}H NMR experiments allowed the assignment of two sets of resonances corresponding to the two coordinated enantiomers (Fig. 3). It is noteworthy that there is a NOE between NH and Hc; inversion at nitrogen is suppressed on coordination to cobalt and the amine hydrogen is located on the same side as the ester group.[10] Similar spectra were obtained for the bis-adducts of *rac*-2-aziridinemethanol, which was obtained by $LiAlH_4$ reduction of *rac*-ethyl 2-aziridinecarboxylate.

Enantiopure (*S*)-ethyl 2-aziridinecarboxylate, prepared by a literature method[11] (see Experimental) gave a set of four resonances upfield of TMS for its $[Co(S)(S)]^+$ bis-adduct. This set is identical to one of the two groups of resonances observed for the *rac*-aziridine (Fig. 4), allowing a complete assignment of the two coordinated enantiomers. The chemical shift differences between the signals of the coordinated enantiomers are very large, up to 0.41 ppm for Ha (Table 3). Hence, **1** appears to be an excellent chiral shift reagent for this type of ligand, and presumably for aziridines in general.

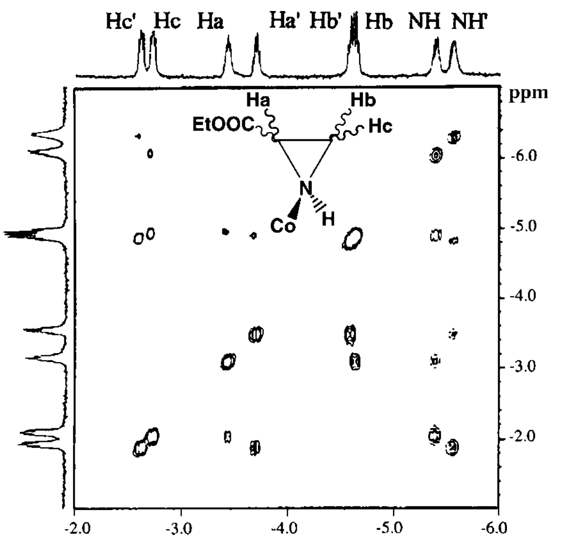

Fig. 3 Two-dimensional ^{1}H NMR spectra (200 MHz, $CDCl_3$) of the bis-adduct of *rac*-ethyl 2-aziridinecarboxylate (upfield region). Above diagonal: NOESYPH; below diagonal: COSY H-H.

^{1}H NMR determination of enantiomer composition of amines

Preliminary experiments were done with racemic mixtures of 1-aminoindane, α-amino-γ-butyrolactone, 1-phenylethylamine, 2-aminomethoxypropane, 2-aziridinemethanol and ethyl 2-aziridinecarboxylate. In every case, the concentration ratio of the two bound enantiomers was found to be equal to 1 within experimental error. The ligands 1-phenylethylamine, 2-aminomethoxypropane and 2-aziridinemethanol exhibited slow exchange, eventually leading to enantioselective binding, similar to that observed previously for β-aminoalcohols.[12] However, enantiomer analysis was reliable if run immediately after addition of the amine derivative.

Several standard solutions of 1-(1-naphthyl)ethylamine covering a range of enantiomer compositions $x = (R)/$

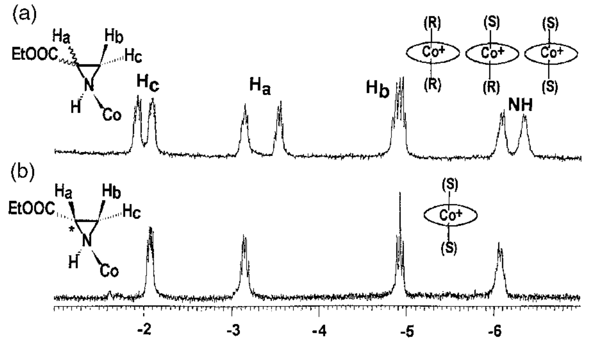

Fig. 4 Upfield ^{1}H NMR resonances (200 MHz) of coordinated *rac*-ethyl 2-aziridinecarboxylate: (a) racemic and (b) enantiopure (*S*).

Table 3 ^{1}H NMR chemical shifts of ethyl 2-aziridinecarboxylate enantiomers in their $Co(TMCP)^+$ bis-adducts

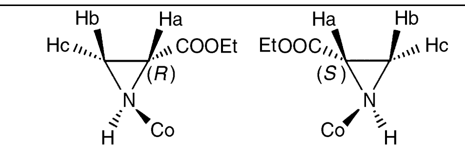

Proton	(*R*)	(*S*)	|Δδ|
Ha	−3.53	−3.12	0.41
Hb	−4.86	−4.94	0.08
Hc	−1.92	−2.08	0.16
NH	−6.34	−6.08	0.26

$[(R) + (S)]$ $(0 \leqslant x \leqslant 1)$ were then analyzed using CoCl(TMCP) as a chiral shift reagent. The determination of the relative composition of bound enantiomers $y = (R_{Co})/[(R_{Co}) + (S_{Co})]$, where $(R_{Co}) = 2[Co(R)(R)]^+ + [Co(R)(S)]^+$ and $(S_{Co}) = 2[Co(S)(S)]^+ + [Co(R)(S)]^+$, was particularly straightforward, by merely integrating the two methyl signals at −2.34 and −2.78 ppm, which exhibit an exceptionally large diastereomeric dispersion; note that $y = x = (R)/[(R) + (S)]$ if amine binding is irreversible (*vide infra*).

The three species $[Co(R)(R)]^+$, $[Co(R)(S)]^+$ and $[Co(S)(S)]^+$ are expected to be formed if $x \neq 0$ or 1, and indeed they are observed. In the lower field region of the spectral window, the 200 MHz NMR profile consists of three sets of peaks for the β-pyrrole protons, including two pairs of singlets for $[Co(R)(R)]^+$ and $[Co(S)(S)]^+$, and a partially overlapping multiplet for $[Co(R)(S)]^+$. In the irreversible regime, $[Co(R)(R)]^+ = x^2$, $[Co(R)(S)]^+ = 2x(1 - x)$ and $[Co(S)(S)]^+ = (1 - x)^2$. A plot of the calculated diastereomer concentrations against the enantiomer composition x is shown in Fig. 5.

Integration of the β-pyrrole resonances could in principle provide experimental values of the relative concentrations of each diastereomer, and thereby a second independent determination of enantiomer composition. However, partial signal overlap makes this analysis much less reliable than that using the amine methyl resonances. Nevertheless, the data points on Fig. 5 are in reasonable agreement with the calculated curves.

The upfield resonances of the CH_3 group of the coordinated 1-(1-naphthyl)ethylamine in non-racemic mixtures are shown in Fig. 6 for standard solutions with $x = 0.25$, 0.5 and 0.75 as representative examples. The experimental values of the enantiomer composition y, measured by integration of the two ligand methyl NMR peaks, are in good agreement with those of x in these cases, as they are also for other values of the composition of the standard solution. The average experimental error $\Delta y/y$ for the seven determinations is 0.6%, and the maximum error is 1.5% for $x = 0.25$ (see Experimental). This good agreement confirms that 1-(1-naphthyl)ethylamine binding on Co(III)(TMCP)$^+$ is irreversible, and that the distribution of the $[Co(R)(R)]^+$, $[Co(R)(S)]^+$ and $[Co(S)(S)]^+$ diastereomers is under kinetic control and depends solely on the enantiomer composition of the amine. Fig. 7(a) shows a plot of the experimental values of y obtained by NMR integration against the composition x of the standard solutions; the linear calibration curve indicates an interesting analytical potential for **1**. Similar experiments were carried out with standard solutions of 2-butylamine. These determinations used the $^1CH_3$ resonances of $[Co(R)(S)]^+$ and $[Co(S)(S)]^+$, which are well-resolved at 400 MHz but not completely at 200 MHz,[7] and they were less precise (average $\Delta y/y < 2\%$, maximum 5% for $x = 0.1$) than in the case of 1-(1-naphthyl) ethylamine but still satisfactory [Fig. 7(b)].

It is therefore apparent that the sensitivity of NMR and

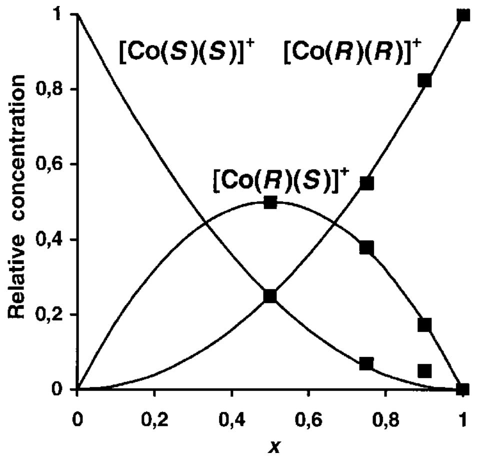

Fig. 5 Calculated concentrations of the three diastereomeric complexes $[Co(R)(R)]^+$, $[Co(R)(S)]^+$ and $[Co(S)(S)]^+$ as a function of the enantiomer composition $x = (R)/[(R) + (S)]$ of standard solutions of 1-(1-naphthyl)ethylamine. Experimental data points are shown as black squares in the range $0.5 \leqslant x \leqslant 1$.

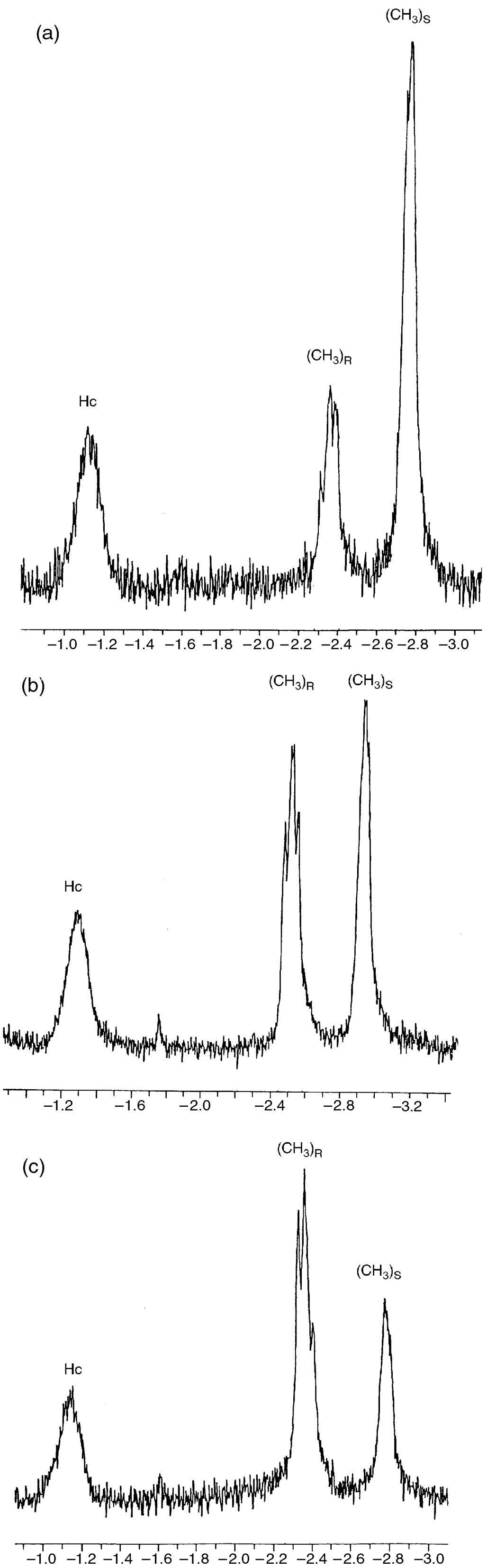

Fig. 6 Upfield resonances of the CH_3 group of coordinated (*R*)- and (*S*)-1-(1-naphthyl)ethylamine for three standard solutions: (a) $(R)/(S) = 0.33$ $(x = 0.25)$; (b) $(R)/(S) = 1$ $(x = 0.5)$; (c) $(R)/(S) = 3$ $(x = 0.75)$.

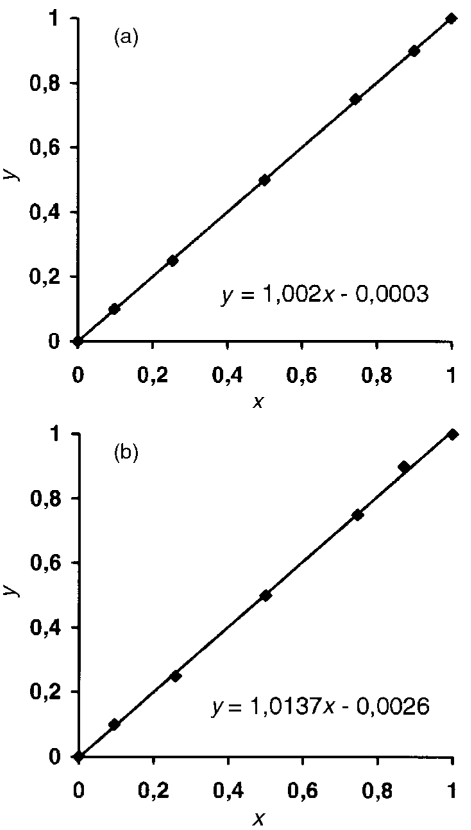

Fig. 7 Plots of the enantiomer composition of cobalt-bound chiral amines, $y = (R_{Co})/[(R_{Co}) + (S_{Co})]$, determined by NMR using CoCl(TMCP) as a chiral shift reagent, against the composition of the standard solutions $x = (R)/[(R) + (S)]$: (a) 1-(1-naphthyl)ethylamine, (b) 2-butylamine.

linear response of the CoCl(TMCP) chiral shift reagent allow the determination of a wide range of enantiomeric compositions with a relative uncertainty of a few percent. Further investigations will be necessary to determine whether this method could be useful for the accurate determination of high enantiomeric purities (beyond 95%), which is difficult by other methods.[13]

X-Ray crystal structures of 2 and 3

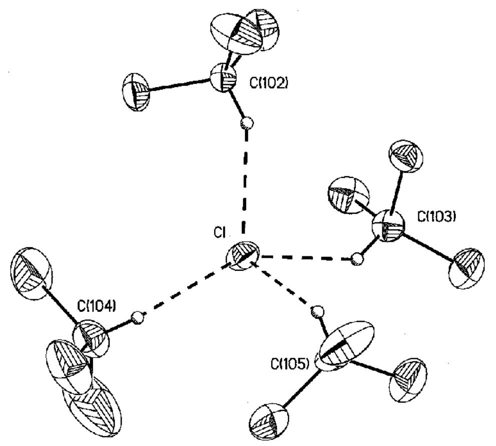

Fig. 9 ORTEP of the chloride anion tetrahedrally coordinated by four chloroform molecules in the crystal of **2**. The four C–H bonds point toward the chloride center within hydrogen-bonding distance. Thermal ellipsoids are at the 30% probability level.

Fig. 8–10 show ORTEP diagrams of the cation and anion of $\{Co[(R)\text{-}1\text{-}(1\text{-naphthyl})ethylamine]_2(TMCP)\}^+Cl^- \cdot 5CHCl_3$, **2**, and of the $\{Co[(R)\text{-}2\text{-butylamine}]_2(TMCP)\}^+$ cation in **3**, respectively. The porphyrin ring of both complexes is ruffled as a result of the αβαβ conformation of the *meso*-cyclopropyl substituents. However, the out-of-plane displacements from the 24-atom macrocyclic mean plane for the four *meso* carbon atoms of the 1-(1-naphthyl)ethylamine complex **2** (average 0.58 Å) are slightly smaller than those found in the analogous (*R*)-2-butylamine complex **3** (0.67 Å) and (*S*)-2-butylamine adduct (0.63 Å).[7] The average Co–N$_p$ distances [1.943(6) Å for **2**, 1.937(6) Å for **3**] are somewhat short compared to other cobalt(III) porphyrins,[14] but similar to those previously reported for ruffled cobalt(III) chiroporphyrins.[7,12,15] The average Co–N$_{ax}$ bond distances [1.997(6) Å for **2**, 1.992(6) Å for **3**] are also consistent with the values previously reported for bis-amine cobalt(III) porphyrins.

The two axial ligands of **2** lie along the chiral grooves that span each face of the porphyrin ring (Fig. 8). The naphthyl planes are not perfectly directed along the C$_{meso}$–C$_{meso}$ axis, probably because of the steric bulk of the methyl group. They are tilted relative to the mean porphyrin plane, with dihedral angles equal to 64.3 and 70.9°. The dihedral angle between the two naphthyl planes is 64.7°. The amine ligands of **2** are held within the porphyrin groove by a network of weak hydrogen-bonding interactions involving the carbonyl groups, in addi-

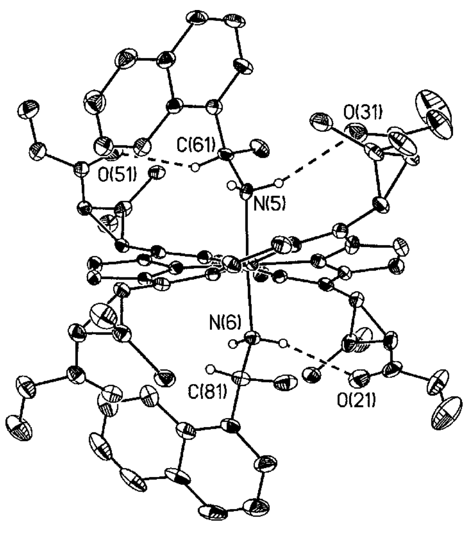

Fig. 8 ORTEP of the structure of the cobalt(III) tetramethylchiroporphyrin-bis[(*R*)-1-(1-naphthyl)ethylamine] cation in **2**. Hydrogen bonds are indicated by dashed lines. Thermal ellipsoids are at the 30% probability level.

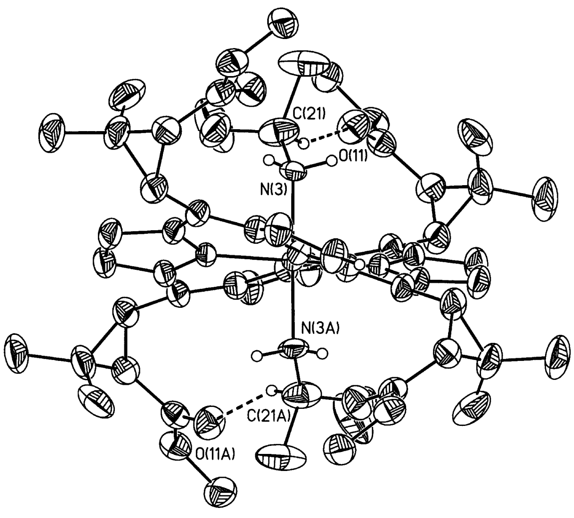

Fig. 10 ORTEP of the structure of the cobalt(III) tetramethylchiroporphyrin-bis[(*R*)-2-butylamine] cation in **3**. Only one orientation of each of the disordered amine ligands is shown. Hydrogen bonds are indicated by dashed lines. Thermal ellipsoids are at the 30% probability level.

Table 4 Crystallographic data for $\{Co[(R)\text{-}1\text{-}(1\text{-naphthyl})ethylamine]_2(TMCP)\}^+Cl^- \cdot 5CHCl_3$, **2** and $\{Co[(R)\text{-}2\text{-butylamine}]_2(TMCP)\}^+Cl^- \cdot 4H_2O$, **3**

	2	**3**
Formula	$C_{77}H_{83}Cl_{16}CoN_6O_8$	$C_{56}H_{84}ClCoN_6O_{12}$
FW	1846.62	1127.67
Crystal system	Triclinic	Hexagonal
Space group	$P1$	$P6_222$
a/Å	11.643 90(10)	11.8042(1)
b/Å	12.7731(2)	11.8042(1)
c/Å	15.5221(3)	38.5292(1)
α/°	81.983(1)	90
β/°	71.1612(1)	90
γ/°	86.863(1)	120
U/Å^3	2163.44(6)	4649.36(6)
Z	1	3
λ/Å	0.710 73	0.710 73
μ/mm^{-1}	0.748	0.380
T/K	193(2)	193(2)
Unique reflect. (R_{int})	10 128(0.0354)	13 067(0.0428)
Indep. reflect. [$I > 2\sigma(I)$]	6546	2308
R_1[a]	0.0632	0.0684
wR_2[a]	0.1576	0.1737

[a] $R_1 = \Sigma \| F_o| - |F_c\| / \Sigma |F_o|$; $wR_2 = [\Sigma w(|F_o| - |F_c|)^2 / \Sigma w F_o{}^2]^{1/2}$; $w = 1/\sigma^2[(F_o)^2 + (0.0501P)^2 + 65.1625P]$ where $P = (F_o{}^2 + 2F_c{}^2)/3$.

tion to the cobalt–nitrogen coordination bond. There is a N–H···O hydrogen bond between Hb on the amine group and a carbonyl group on each face of the porphyrin [N(6)–H(6B)···O(21) 2.533(2) Å]. Furthermore, the hydrogen atom Hc on the asymmetric carbon is involved in a weak C–H···O hydrogen bond to the second carbonyl group on one face [C(61)–H(61)···O(51) 2.424(3) Å] and a weaker one on the other [C(81)–H(81)···O(41) 2.751(2) Å]. Similar C–H···O contacts involving Hc are found in the structure of the (*R*)-2-butylamine adduct **3** [C(21)–H(21)···O(11) 2.29(1) Å] (Fig. 10).

The chloride counter-anion of **2** is surrounded by four chloroform molecules, which sit on the apices of a distorted tetrahedron (Fig. 9), with the four C–H bonds pointing toward the center within hydrogen-bonding distances[16] [C(102)–H(102)···Cl 2.588(5); C(103)–H(103)···Cl 2.445(6); C(104)–H(104)···Cl 2.452(6); C(105)–H(105)···Cl 2.646(6) Å].

Conclusion

CoCl(TMCP) is a convenient chiral metalloporphyrin shift reagent for primary amine and aziridine derivatives. Derivatization is carried out in the NMR tube at room temperature using a few µmol of amine, and the diastereomeric products are obtained in quantitative yields for both enantiomers. In the case of 1-(1-naphthyl)ethylamine and ethyl 2-aziridinecarboxylate, the analyte exhibits narrow ^{1}H NMR lines, which are shifted to a vacant spectral window upfield of TMS. The large diastereomeric dispersion allows the use of a standard 200 MHz spectrometer for analysis. The practical determination involves integration of two well-resolved peaks and is therefore quick and easy. The instrumental response is linear over the entire range of enantiomer composition. These features of CoCl(TMCP) make it a promising chiral shift reagent for the determination of the enantiomeric composition of amines and aziridines.

Experimental

Materials and methods

Chloro(tetramethylchiroporphyrin)cobalt(III) CoCl(TMCP) was prepared according to a procedure worked out earlier in our laboratories.[7,17] Chiral amines of the highest available enantiomer ratio were purchased from Fluka: (*R*)- and (*S*)-1-(1-naphthyl)ethylamine, er > 99.5 : 0.5 (ChiraSelect); (*R*)- and (*S*)-2-butylamine ($[\alpha]_D^{20} = \pm 7.5°$), and were used as received. Racemic amines were from Aldrich.

Racemic ethyl 2-aziridinecarboxylate was prepared from ethyl α-bromoacrylate and ammonia according to a previously described method.[11a,b] Enantiopure (*S*)-ethyl 2-aziridinecarboxylate was prepared in three steps from the ethyl ester of L-serine.[11c,d]

^{1}H NMR spectra were recorded on Bruker 200 MHz or Varian 400 MHz NMR spectrometers. Parameters for acquiring proton spectra were the following: Bruker 200 MHz, 16 accumulations, spectral window 4000 Hz, 16 K data points; Varian 400 MHz, 8 accumulations, spectral window 8000 Hz, 58.5 K data points. Chemical shifts are reported relative to TMS.

^{1}H NMR analysis of enantiomer composition

Standard solutions of 1-(1-naphthyl)ethylamine in $CDCl_3$ of various enantiomer ratios (<1 : 99, 10 : 90, 25 : 75, 50 : 50, 75 : 25, 90 : 10, >99 : 1) at a total concentration of 2.1 M were prepared by mixing appropriate volumes of each enantiopure compound (typically 15 to 150 µL) in 0.5 mL of $CDCl_3$. A 10 µL aliquot of the standard solution (6 equiv.) was then added to a solution of 3.3 mg (3.5 µmol) of CoCl(TMCP) in $CDCl_3$ (0.7 mL) in an NMR tube. The formation of the bis-adduct salt was immediate. ^{1}H NMR spectra were taken immediately following addition and 24 h later.

The difficulty of accurate sampling of µL volumes of enantiopure amine can be a problem in the preparation of standard solutions of chiral amine in $CDCl_3$, as it can result in a larger experimental error for solutions of lower concentration of S ($x > 95\%$) or R ($x < 5\%$). Fast solvent evaporation is another source of experimental uncertainty in this concentration range. Thus, the experimental errors observed in the calibration curves are likely to reflect the uncertainties in the preparation of standard solutions, rather than the intrinsic accuracy of the analytical method.

X-Ray crystal structure determinations

Single crystals were obtained by slow diffusion of *n*-hexane in 0.7 mL of a $CDCl_3$ solution of **2** or **3** used for NMR studies. A summary of crystallographic data is shown in Table 4.

Data were collected on a three-circle diffractometer equipped with a Siemens SMART CCD area detector using graphite-monochromated Mo-Kα radiation. Programs used were SAINT (data collection),[18] SADABS (absorption correction)[19] and SHELXTL 5.1 (structure solution).[20] Cell parameters were obtained with intensities detected on three batches of 15 frames with a 10 s exposure time for each, and were refined using unique intensities with $I > 10\sigma(I)$ from all data. The structures were solved by direct methods using the SHELXTL package. All non-hydrogen atoms were found by difference Fourier syntheses and were refined anisotropically on F^2. Hydrogen atoms were treated as riding atoms.

CCDC reference numbers 104406 and 159943. See http://www.rsc.org/suppdata/nj/b1/b100268f/ for crystallographic data in CIF or other electronic format.

Acknowledgements

We thank Françoise Sarrazin and Pierre-Alain Bayle for assistance with the Varian 400 MHz spectrometer.

References and notes

1 R. Sheldon, *Chirotechnology: Industrial Synthesis of Optically Active Compounds*, Dekker, New York, 1993.

2 For recent reviews, see: (*a*) H. Y. Aboul-Enein, *Anal. Lett.*, 1988, **21**, 2155; (*b*) D. Parker, *Chem. Rev.*, 1991, **91**, 1441; (*c*) A. F. Casy,

Trends Anal. Chem., 1993, **12**, 185; (*d*) E. L. Eliel and S. H. Wilen, *Stereochemistry of Organic Compounds*, Wiley, New York, 1994, p. 221; (*e*) B. A. Dawson and G. L. Mattok, *Pharmeuropa*, 1997, **9**, 347; (*f*) R. Rothchild, *Enantiomer*, 2000, **5**, 457.

3 For examples, see: (*a*) W. H. Pirkle and K. A. Simmons, *J. Org. Chem.*, 1981, **46**, 3239; (*b*) A. Nabeya and T. Endo, *J. Org. Chem.*, 1988, **53**, 3358; (*c*) S. Miyano, S. Okada, H. Hotta, M. Takeda, T. Suzuki, C. Kabuto and F. Yasuhara, *Bull. Chem. Soc. Jpn.*, 1989, **62**, 3886; (*d*) R. Hulst, R. W. J. Zijlstra, B. L. Feringa, N. Koen de Vries, W. Ten Hoeve and H. Wynberg, *Tetrahedron Lett.*, 1993, **34**, 1339; (*e*) S. Hamman, *J. Fluorine Chem.*, 1993, **60**, 225; (*f*) A. Alexakis, J. C. Frutos, S. Mutti and P. Mangeney, *J. Org. Chem.*, 1994, **59**, 3326; (*g*) K. Nagasawa, A. Yamashita, S. Katoh, K. Ito and K. Wada, *Chem. Pharm. Bull.*, 1995, **43**, 344; (*h*) R. Wu, G. Hernandez, J. D. Odom, R. B. Dunlap and L. A. Silks, *Chem. Commun.*, 1996, 1125; (*i*) R. Chinchilla, L. R. Falvello and C. Najera, *J. Org. Chem.*, 1996, **61**, 7285; (*j*) T. J. Wenzel, A. C. Bean and S. L. Dunham, *Magn. Reson. Chem.*, 1997, **35**, 395; (*k*) K. Nagasawa, R. Okazaki, A. Yamashita, K. Ito and K. Wada, *Heterocycles*, 1997, **45**, 1047.

4 For examples, see: (*a*) D. Greatbanks and R. Pickford, *Magn. Reson. Chem.*, 1987, **25**, 208; (*b*) S. C. Benson, P. Cai, M. Colon, M. A. Haiza, M. Tokles and J. K. Snyder, *J. Org. Chem.*, 1988, **53**, 5335; (*c*) D. Parker and R. J. Taylor, *Tetrahedron*, 1987, **43**, 5451; (*d*) R. Chinchilla, F. Foubelo, C. Najera and M. Yus, *Tetrahedron: Asymmetry*, 1995, **6**, 1877; (*e*) J. Omelanczuk and M. Mikolajczyk, *Tetrahedron: Asymmetry*, 1996, **7**, 2687; (*f*) M. Thunhorst and U. Holzgrabe, *Magn. Reson. Chem.*, 1998, **36**, 211; (*g*) M. Sarfati, P. Lesot, D. Merlet and J. Courtieu, *Chem. Commun.*, 2000, 2069.

5 For reviews, see: (*a*) A. F. Cockerill, G. L. Davies, R. C. Harden and D. M. Rackham, *Chem. Rev.*, 1973, **73**, 553; (*b*) G. R. Sullivan, *Top. Stereochem.*, 1978, **10**, 287; (*c*) V. Schurig, *Kontakte* (*Darmstadt*), 1985, 22. See also: S. E. Weinstein, M. S. Vining and T. J. Wenzel, *Magn. Reson. Chem.*, 1997, **35**, 273.

6 (*a*) D. B. Grothjan and C. Joubran, *Tetrahedron: Asymmetry*, 1995, **6**, 745; (*b*) B. Staubach and J. Buddrus, *Angew. Chem., Int. Ed. Engl.*, 1996, **35**, 1344.

7 D. Toronto, F. Sarrazin, J. Pécaut, J. C. Marchon, M. Shang and W. R. Scheidt, *Inorg. Chem.*, 1998, **37**, 526.

8 $[\mathrm{Co}(R)(R)]^+$, $[\mathrm{Co}(R)(S)]^+$ and $[\mathrm{Co}(S)(S)]^+$ are abbreviations for the $[(\mathrm{TMCP})\mathrm{Co}]^+$ adducts with two (*R*), one (*R*) and one (*S*), and two (*S*) axial ligands, respectively.

9 M. Mazzanti, M. Veyrat, R. Ramasseul, J. C. Marchon, I. Turowska-Tyrk, M. Shang and W. R. Scheidt, *Inorg. Chem.*, 1996, **35**, 3733.

10 For a similar case see: D. C. Ware, B. G. Siim, K. G. Robinson, W. A. Denny, P. J. Brothers and G. R. Clark, *Inorg. Chem.*, 1991, **30**, 3750.

11 (*a*) E. Kyburz, H. Els, S. Majnoni, G. Englert, C. von Planta, A. Fürst and P. A. Plattner, *Helv. Chim. Acta*, 1966, **49**, 359; (*b*) M. Bucciarelli, A. Forni, I. Moretti, F. Prati and G. Torre, *J. Chem. Soc., Perkin Trans. 1*, 1993, 3041; (*c*) E. Kuyl-Yeheskiely, M. Lodder, G. A. van der Marel and J. H. van Boom, *Tetrahedron Lett.*, 1992, **33**, 3013; (*d*) K. Nakajima, F. Takai, T. Tanaka and K. Okawa, *Bull. Chem. Soc. Jpn.*, 1978, **51**, 1577.

12 J.-P. Simonato, J. Pécaut and J.-C. Marchon, *J. Am. Chem. Soc.*, 1998, **120**, 7363.

13 A. K. Gupta and R. J. Kazlauskas, *Tetrahedron: Asymmetry*, 1992, **3**, 243.

14 W. R. Scheidt, *Acc. Chem. Res.*, 1977, **10**, 339.

15 J.-P. Simonato, J. Pécaut and J.-C. Marchon, *Inorg. Chim. Acta*, 2000, **304**, 288.

16 T. Steiner, *Acta Crystallogr., Sect. B*, 1998, **54**, 456.

17 C. Pérollier, M. Mazzanti, J.-P. Simonato, F. Launay, R. Ramasseul and J.-C. Marchon, *Eur. J. Org. Chem.*, 2000, 583.

18 SMART and SAINT, Area Detector Control and Integration Software, Siemens Analytical X-Ray Instruments Inc., Madison, WI, USA, 1995.

19 SADABS, Bruker Area Detector Absorption Corrections Software, Bruker Analytical X-Ray Systems, Wissembourg, France, 1998.

20 G. M. Sheldrick, SHELXTL-Plus, Structure Determination Software, Siemens Analytical X-Ray Instruments Inc., Madison, WI, USA, 1998.